URBAN GROWTH ASSESSMENT AND ITS IMPACT ON DEFORESTATION IN BAUCHI METROPOLIS, NIGERIA USING REMOTE SENSING AND GIS TECHNIQUES

Sulaiman Ibrahim Musa[1, 2, 3], Mazlan Hashim[1, 2] and Mohd Nadzri Md Reba[1, 2]

[1]Geoscience and Digital Earth Centre, Research Institute for Sustainable Environment, Universiti Teknologi Malaysia, Johor, Malaysia
[2]Faculty of Geoinformation and Real Estate, Universiti Teknologi Malaysia, Johor Bahru, Malaysia
[3]Department of Surveying and Geoinformatics, Abubakar Tafawa Balewa University, Bauchi, Bauchi State, Nigeria
E-Mail: sulaimanibrahimmusa@gmail.com

ABSTRACT

Urban areas are rapidly expanding due to population growth and development, leading to deforestation and land degradation. This study employed remote sensing and GIS techniques to assess urban growth and its impact on deforestation in Bauchi metropolis, Nigeria within the last three decades (1986-2016). The study made use of Landsat images of four epochs; Thematic Mapper (TM) of 1986 and 1996, Enhanced Thematic Mapper of 2006, and Operational Land Imager (OLI) of 2016. Color compositions were made after which the images were geometrically and radiometrically restituted. The images were classified using maximum likelihood algorithm and the accuracy of the classification was assessed by cross-validation using confusion matrices and ground truthing by the use of a hand-held Global Positioning System (GPS). The classified images with their kappa indexes were TM of 1986 (0.83%) and 1996 (0.87%), ETM+ of 2006 (0.90%) and OLI of 2016 (0.92%), respectively. Post-classification comparisons and analyses were performed and the results revealed that changes have taken place in bare surface (+32.43%), built-up area (+565.24%), farm land (+66.42%), forest (-91.80%) and rock outcrop (-49.21%) in the metropolis between 1986 and 2016. The land cover features of the metropolis were reclassified into forest and non-forest for cross-tabulation analysis and the result of the analysis indicates a change-over of 14965.97Ha (39.68%) form forest to non-forest (deforestation) and that of 467.69Ha (1.24%) form non-forest to forest (afforestation) between 1986 and 2016. This shows a rapid increase in built-up area (urban growth) and rapid decrease in forest (deforestation), which may be attributed to lack of improper environmental protection strategy in place in the metropolis. The study demonstrates the potentialities of remote sensing and GIS in assessing urban growth and its impacts on deforestation. The outcome of the study can serve as input into a relationship model for predicting the impact of urban growth on deforestation.

Keywords: urban growth, deforestation, afforestation, land cover, change detection.

INTRODUCTION

Urban areas are rapidly expanding in both developed and developing nations [1, 2]. However, urban land expansion is placing a formidable challenge in many countries around the globe, especially in terms of deforestation and land degradation [3]. Presently, more people dwell in urban areas than rural areas [4], and about 40 percent of the world's people lives in dry lands accounting for about 20 percent of the earth's surface [5]. In spite of the fact that urbanization remains a key to modernization, economic growth and development, it equally has some reverberations on the environment [6, 7]. Looking at the influence of urban growth on deforestation, it becomes imperative to understand how urban areas are developing and the impacts of their development on the physical environment especially in terms of biodiversity and land degradation.

Even though, numerous attempts have been made to assess urban growth in the last few decades [8, 9] and its impacts on the environment [6, 10] but assessing the impacts of urban growth on deforestation is not given much attention by the researchers. Where there is deforestation, as in the case of Bauchi metropolis, decision making for proper environmental management strategy would require knowledge of the magnitude of the deforestation and where it has taken place but this remains a challenging issue. This study therefore seeks to employ remote sensing and GIS techniques to assess urban growth and its impacts on deforestation using Bauchi metropolis as a case study.

STUDY AREA

Bauchi metropolis, the administrative headquarters of Bauchi State, is situated in the north eastern Nigeria. It covers an area of 632 sqkm and geographically located between latitudes 10° 12′ and 10° 27′ North of the Equator and longitudes 9° 40′ and 9° 57′ East of the Greenwich Meridian (Figure-1). It is connected by good roads, lies on the Nigeria's major rail line that links Maiduguri and Port Harcourt, and serves as an entrance to the north-eastern states that include Bauchi, Yobe, Gombe, Adamawa, Taraba and Borno.

There are two seasons that mark the climate condition of the metropolis; a dry season that lasts from October to April (about seven months) when humidity is between 12% and 36%, and a wet season that lasts from May to September (about five months) when humidity is between 37% and 68%, with a mean annual rainfall of 1091.4mm [11]. The temperatures of the metropolis are between 13.3°C in December and 22.1°C in May (minimum) and between 28.2°C in August and 36.6° in April (maximum) [12]. The metropolis is situated within

www.arpnjournals.com

the belt of open Sudan savannah, characterized by sparse trees of up to 20ft or more, and had a projected population of over 318,038 people in 2016 [13].
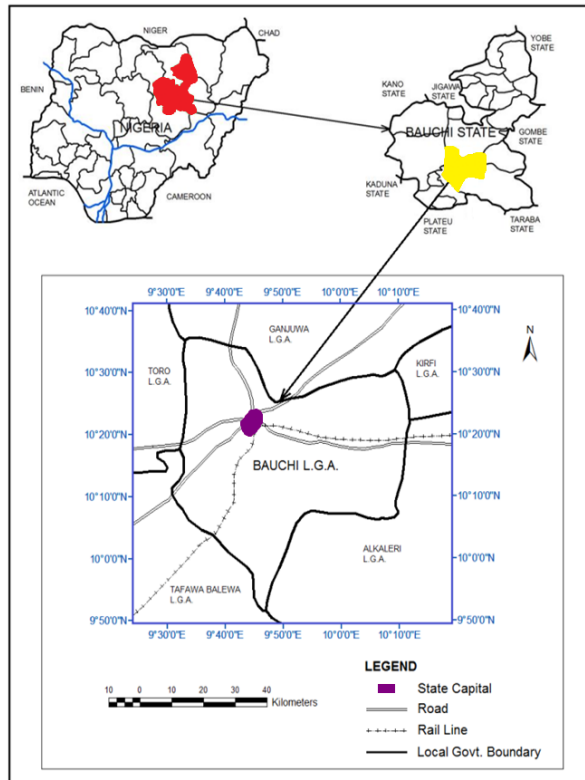

Figure-1. The study area.

MATERIALS AND METHODS

Materials

Multitemporal satellite images (Landsat) of four epochs; Thematic Mapper (TM) of 1986 and 1996, Enhanced Thematic Mapper (ETM+) of 2006 and Operational Land Imager (OLI) of 2016, topographical map (2008 version) of Bauchi N. E. sheet 149 (1:50,000), training samples, and land use maps were utilized in this study. The images were obtained from the Earth Resources Observation System (EROS) Data Centre of the U.S.G.S. and topographical/land use maps from the Bauchi State Ministry of Land and Survey, while training samples were obtained though field survey using GPS. The TM images of 1986 and 1996 were acquired on November 6 and December 20, respectively while the ETM+ of 2006 and OLI of 2016 on December 2 and November 27, respectively. IDRISI Selva and ArcGIS 10.3 were the software packages used in the study.

Methods

The methodology employed comprises the following phases; data collection, image enhancement, image classification, urban growth/land cover change analyses and deforestation assessment. Figure-2 describes the methodological framework adopted. In image enhancement phase, geometric and radiometric restitutions of the four sets of Landsat images were performed. In image classification phase, the images were classified, after generating training samples, by supervised classification using maximum likelihood algorithm. In the urban growth/land cover change analyses phase, post-classification comparisons and analyses were performed to reveal the urban growth/land cover change pattern in the study area. In the last phase, deforestation assessment, image re-classification and cross-tabulation analysis were performed to assess the extent of deforestation in the study area.
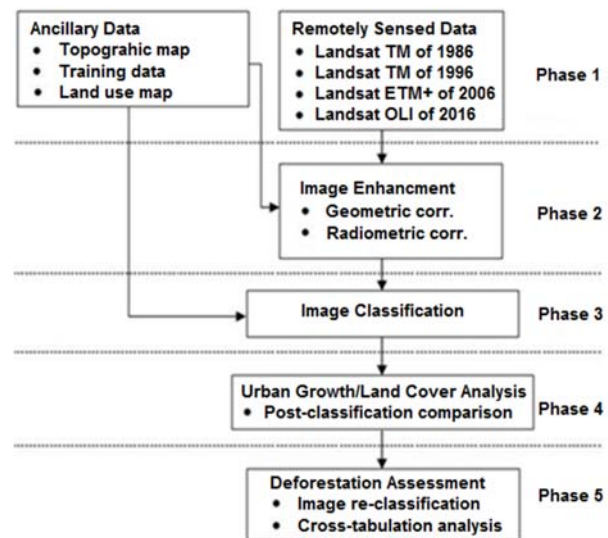

Figure-2. The methodological framework.

RESULTS AND DISCUSSIONS

Image enhancement

It is very crucial to perform image pre-processing or enhancement in remote sensing in order to remove or reduce the noises and distortions introduced at the time of imaging. This will force the images' radiometric and geometric characteristics to be like that of the original scene's radiant energy [14]. For this study, two corrections were applied to the raw satellite images, namely; geometric and radiometric. The corrections and their results are presented below.

Radiometric correction

This study utilized Empirical Line Calibration to transform the radiance recorded by the sensor to reflectance [15-17]. The reflectance of two sets of targets identified on the ground, from dark and light areas, was measured. The average spectra of the same sets of targets were extracted after identifying them on the Landsat TM of 1986 (one of the four images). For each band, a linear relationship for transforming radiance to reflectance was derived using regression analysis. The following formulae were employed to generate gains and offsets used to arrived at pixel-by-pixel apparent reflectance [15].

$$\text{Reflectance} = \text{Gain (K)} \times \text{Radiance} + \text{Offset (b)} \quad\text{......... (1)}$$

Where

$$K = \frac{N \sum (DN_i r_i) - \sum r_i \sum DN_i}{N \sum r_i^2 - (\sum r_i)^2} \qquad (2)$$

$$b = \frac{\sum DN_i r_i^2 - K \sum r_i^2}{\sum r_i} \qquad (3)$$

The gain and offset stood at 1.0399 and 153.00, respectively. After substituting these values, Equation (1) becomes $y = 1.0399x - 153.00$ with an R^2 value of 0.9533. Calibration of reflectance was performed by utilizing the regression value generated using the equations above which leads to atmospherically restituted image and the same procedure was adopted for the images of 1996, 2006 and 2016 (Figure-3).
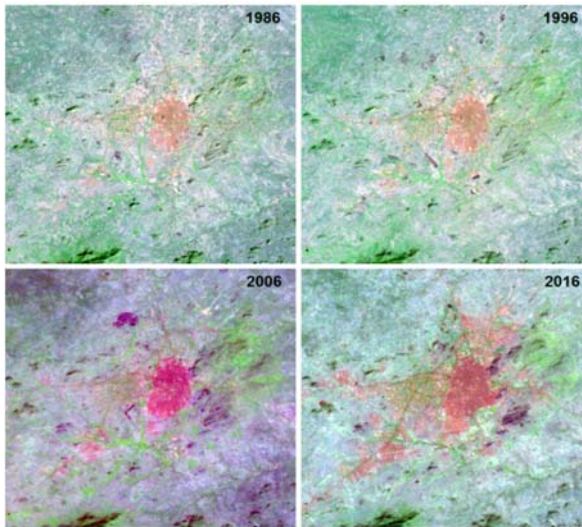

Figure-3. Radiometrically corrected images.

Geometric correction

Image-to-map rectification using tallying ground control points in both the image and topographic map was the geometric correction approach employed to rectify the 1986 image [18]. This allows for ascertaining the potency of pixel transposition from image to map grid. The image was geometrically calibrated using 30 ground control points. The respective pixel coordinates of each control point in the image were used to compute its UTM coordinates. These UTM coordinates and those obtained from the map were then compared and the differences (errors) calculated in two directions, Easting and Northing. The following equations were used to compute root mean squired errors in the two directions so as to have an overall picture of the calibration accuracy.

$$RMSE_x = [\frac{1}{n} \sum_{i=1}^{n} (\delta x_i)^2]^{\frac{1}{2}} \qquad (4)$$

Where $RMSE_x$ = root mean squared error in x direction, n = number of GCPs and δx_i = residual of the ith GCP.

$$RMSE_y = [\frac{1}{n} \sum_{i=1}^{n} (\delta y_i)^2]^{\frac{1}{2}} \qquad (5)$$

Where $RMSE_y$ = root mean squared error in y direction, n = number of GCPs and δy_i = residual of the ith GCP.

A planimetric $RMSE$ ($RMSE_{xy}$) was formed by matching $RMSE_x$ and $RMSE_y$, using the following formulae:

$$RMSE_{xy} = [RMSE_x^2 + RMSE_y^2]^{\frac{1}{2}} \qquad (6)$$

The root mean squared error (RMSE) of the geometric rectified image (TM of 1986) was found to be 0.501 of pixel dimension or 15.03m.

After the 1986 image was geometrically rectified, image registration was employed where the 1986 image was used as a reference/source image to rectify those of 1996, 2006 and 2016.

Image Classification

The four sets of images were classified, after generating training samples, using maximum likelihood classifier by supervised classification [19, 20]. Six land covers were classified, which include bare surface, built-up area, farmland, forest and rock outcrop. Cross-validation statistics using confusion matrix was employed to assess the classification accuracy. Table-1 presents the classified images with their overall accuracies/Kappa indexes. The accuracy was also ascertained using field validation with the help of a hand-held GPS and an agreement was found between the classified land covers and ground features.

Table-1. Classified images with their overall accuracies and Kappa indexes.

Image	Overall accuracy (%)	Kappa index
Landsat TM of 1986	86.89	0.83
Landsat TM of 1996	89.47	0.87
Landsat ETM+ of 2006	92.33	0.90
Landsat OLI of 2016	94.32	0.92

The accuracy assessment shows that the acceptable range of more than 85 percent was achieved and this may be attributed to the use of five land covers

only [21]. This also shows that the fewer land cover classified the higher the classification accuracy.

Urban growth/Land cover (LC) Change analysis

Post-classification comparison

The potencies of using remotely sensed imageries and ground survey in acquiring training samples were proven for detecting changes in land cover in the study area as within the last three decades (1986-2016) shown in Figure-4.

Table-2 and Figure-5 present the land cover changes derived from the comparative analysis of the classified images of the study area, from 1986 to 2016.
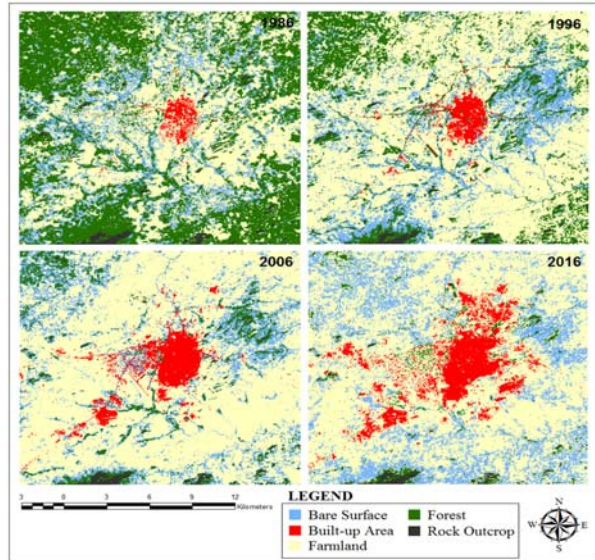

Figure-4. Land cover maps of 1986, 1996, 2006 and 2016.

Table-2. Land cover of the study area, 1986 to 2016.

| Land cover categories	1986		1996		2006		2016	
	Area (Ha)	Area (%)	Area (Ha)	Area (%)	Area (Ha)	Area (%)	Area (Ha)	Area (%)
Bare Surface	5715.45	15.15	6161.67	16.34	7072.31	18.75	7569.00	20.07
Built-up Area	525.87	1.39	1006.02	2.67	2993.09	7.94	3498.30	9.28
Farmland	15038.73	39.87	23359.86	61.94	24757.36	65.64	25027.29	66.36
Forest	15793.56	41.87	6754.59	17.91	2481.48	6.58	1295.46	3.43
Rock Outcrop	643.05	1.71	434.52	1.15	412.42	1.09	326.61	0.87
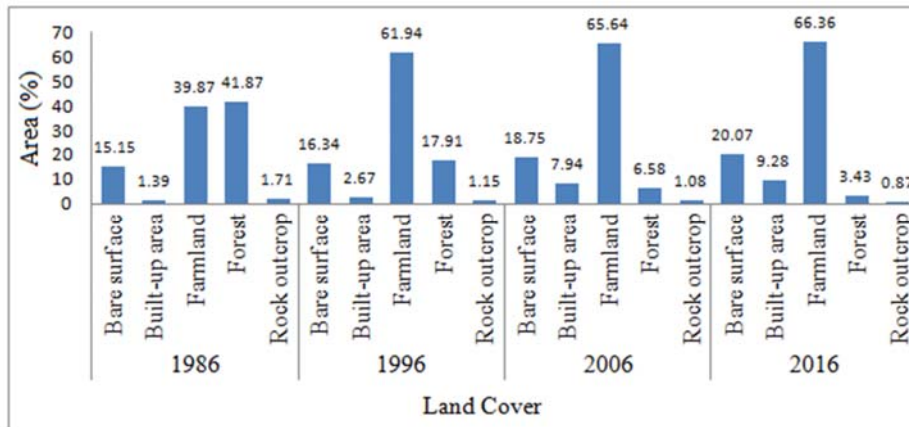
Figure-5. Distribution of land cover, 1986 to 2016.

From Table-3, it can be seen that a remarkable increase in built-up area (565.24%) has occurred in the study area during the last thirty years. Farmland and bare surface have also experienced positive changes of +66.42% and +32.43%, respectively. Likewise, forest and rock outcrop, where negative changes of -49.21% and -91.80% were observed.

These changes especially the increment in bare surface/farmland and reduction in forest may not be unconnected with transition from forest to farmland as well as unreasonable vanishing of trees for firewood. This is largely due to over dependency on firewood as the major source of energy for cocking in the metropolis.

www.arpnjournals.com

Table-3. LC and LU changes, 1986 to 2016.

Land cover categories	1986-1996		1996-2006		2006-2016		1986-2016	
	Change (Ha)	Change (%)	Change (Ha)	Change (%)	Change (Ha)	Change (%)	Change (Ha)	Change (%)
Bare Surface	446.22	7.81	910.64	14.78	6496.69	91.86	1853.55	32.43
Built-up Area	480.15	91.31	1987.07	197.52	505.21	16.88	2972.43	565.24
Farmland	8321.13	55.33	1397.50	5.98	269.91	1.09	9988.56	66.42
Forest	-9038.97	-57.23	-4273.11	-63.26	-1186.02	-47.79	-14498.10	-91.80
Rock Outcrop	-208.53	-32.43	-22.10	-5.09	-85.81	-20.81	-316.44	-49.21

Moreover, the increment in built-up area may be associated with rapid population growth due to rural-urban drift which in turn leads to housing and infrastructural development in the area. Thus, it can be asserted that the built-up area's increment is a sign of urban growth, which at the same time pressurised the available resources.

Deforestation assessment

In order to assess the impact of urban growth on deforestation in the study area, image re-classification and cross-tabulation analysis where performed.

Image Re-classification

The 1986, 1996, 2006 and 2016 land cover classes of the study area were re-classified into two land cover classes, forest and non-forest. The bare surface, built-up area, farmland and rock outcrop were merged together to form a non-forest land cover while the forest land cover remained as it was. The re-classification result was presented in Figure-6 and tabulated in Table-4.

Table-4. Forest and non-forest land cover of the study area, 1986 to 2016.

Land cover categories	1986		1996		2006		2016	
	Area (Ha)	Area (%)	Area (Ha)	Area (%)	Area (Ha)	Area (%)	Area (Ha)	Area (%)
Forest	15793.56	41.87	6754.59	17.91	2481.48	6.58	1295.46	3.43
Non-forest	21923.10	58.13	30962.07	82.09	35235.18	93.42	36421.20	96.57
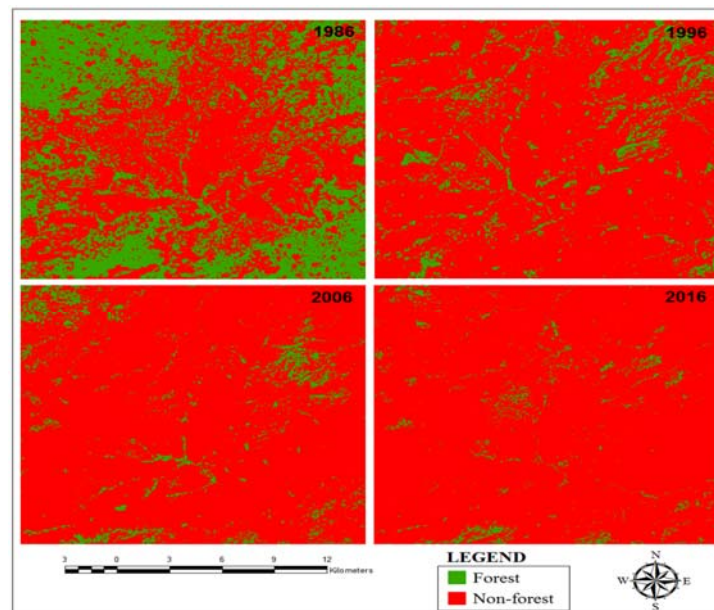
Figure-6. Re-classified land covers, 1986 to 2016.

www.arpnjournals.com

Cross-tabulation analysis

In order to ascertain the magnitude of the deforestation and where is has taken place, between 1986 and 2016, in the metropolis; cross-tabulation analysis was conducted by establishing pixel-to-pixel changes from the re-classified images of the two periods. The cross-tabulation result is presented and interpreted in Table 6 and Figure-7.

The accuracy of the re-classification and cross-tabulation was ascertained through field validation using a hand-held GPS. A strong agreement was observed between what is on the re-classification/cross-tabulation maps and ground features.

Table-5. Interpretation of the change-over between forest and non-forest, 1986-2016.

| S. N	Result	Area (Ha)	Area (%)	Interpretation of result	Remark
1	1|1	825.99	2.19	Forest in 1986 and remained forest in 2016	Unchanged
2	2|1	467.69	1.24	Non-forest in 1986 and turned to forest in 2016	Afforestation
3	1|2	14965.97	39.68	Forest in 1986 and turned to non-forest in 2016	Deforestation
4	2|2	21457.01	56.89	Non-forest in 1986 and remained non-forest in 2016	Unchanged

Key: 1 = Forest; 2 = Non-forest
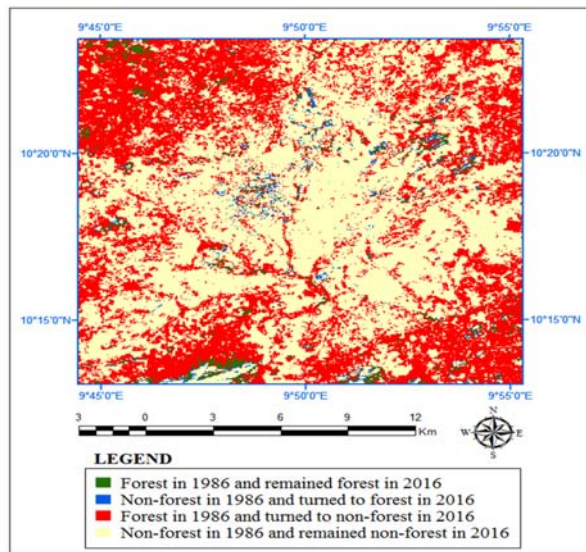
Figure-7. Land covers conversion, 1986-2016.

CONCLUSIONS

Recent development in technology has eased the acquisition of data for different kinds of studies. With this development, remote sensing and GIS have become potent techniques for generating and analysing geospatial data about geographical features. This study made use of multitemporal Lands at satellite images of four epochs; TM of 1986 and 1996, ETM+ of 2006, and OLI of 2015 to assess urban growth and its impacts on deforestation in Bauchi metropolis, Bauchi Sate, Nigeria over a period of thirty years (1986-2016). The Lands at imagery was chosen for this study because of its open source (free access) coupled with temporal availability. The empirical line calibration and image-to-map methods used for radiometric and geometric restitution of the images as well as maximum likelihood algorithm for image classification have proved their effectiveness in enhancing the images and classifying the features within the metropolis. The accuracy of the classification was assessed by cross-validation using confusion matrices and the kappa indexes of the four classified images were 0.83%, 0.87%, 0.90% and 0.92% for the TM of 1986 and 1996, ETM+ of 2006, and OLI of 2016, respectively. Ground truthing by the use of a hand-held Global Positioning System (GPS) was also conducted as a field validation to assess the classification accuracy and the result shows a strong agreement between the ground features and those on the classified images. For higher classification accuracy and better assessment, satellite images of higher resolution such as WorldView or GeoEye and more powerful feature extraction algorithms such as object oriented should be used for future studies.

The post-classification comparisons and Paired t-test analyses performed in the study uncovered significant changes in bare surface (+32.43%), built-up area (+565.24%), farm land (+66.42%), forest (-91.80%) and rock outcrop (-49.21%) in the metropolis between 1986 and 2016. After reclassifying the land cover features of the metropolis into forest and non-forest and performing cross-tabulation analysis, the result of indicates a change-over of 14965.97Ha (39.68%) form forest to non-forest (deforestation) and that of 467.69Ha (1.24%) from non-forest to forest (afforestation) within the study period. The rapid increase in built-up area indicates urban growth while the decrease in forest indicates deforestation. The deforestation may be attributed to lack of proper environmental protection strategy in place in the metropolis and if allowed to be continued like that in the future, it will have great repercussion on the metropolis. The study demonstrates the potentialities of remote sensing and GIS in assessing urban growth and its impacts on deforestation, and the outcome of the study can serve as an input into a relationship model for predicting the impact of urban growth on deforestation.

ARPN Journal of Engineering and Applied Sciences

REFERENCES

[1] M. Al-shalabi, L. Billa, B. Pradhan, S. Mansor and A. A. Al-Sharif. 2013. Modelling urban growth evolution and land-use changes using GIS based cellular automata and SLEUTH models: the case of Sana'a metropolitan city, Yemen. Environmental earth sciences. 70: 425-437.

[2] S. I. Musa, M. Hashim, and M. N. M. Reba. 2016. A review of geospatial-based urban growth models and modelling initiatives. Geocarto International. 31: 1-21.

[3] M. Reed and L. C. Stringer. 2015. Climate change and desertification: Anticipating, assessing & adapting to future change in drylands. Impulse Report for the 3rd UNCCD Scientific Conference on: Combatung desertification/land degradation and drought for poverty reduction and sustainable development: the contribution of science, technology, traditional knowledge and practice. 9-12 March 2015, Cancun, Mexico. Montpellier: Agropolis International.

[4] 2014. UN, World Urbanization Prospects. The 2014 Revision. New York, NY: United Nations.

[5] R. P. White and J. Nackoney. 2003. Drylands, people, and ecosystem goods and services: A web-based geospatial analysis. Washington, DC: World Resources Institute (WRI).

[6] Y. D. Wei and X. Ye. 2014. Urbanization, urban land expansion and environmental change in China. Stochastic Environmental Research and Risk Assessment. 28: 757-765.

[7] S. Townroe and A. Callaghan. 2014. British Container Breeding Mosquitoes: The Impact of Urbanisation and Climate Change on Community Composition and Phenology. PLOS ONE. 9: 1-7.

[8] J. J. Arsanjani, M. Helbich and E. de Noronha Vaz. 2013. Spatiotemporal simulation of urban growth patterns using agent-based modeling: the case of Tehran. Cities. 32: 33-42.

[9] Y. Xie and S. Fan. 2014. Multi-city sustainable regional urban growth simulation-MSRUGS: a case study along the mid-section of Silk Road of China. Stochastic Environmental Research and Risk Assessment. 28: 829-841.

[10] D. Grawe, H. L. Thompson, J. A. Salmond, X. M. Cai and K. H. Schlünzen. 2013. Modelling the impact of urbanisation on regional climate in the Greater London Area. International Journal of Climatology. 33: 2388-2401.

[11] WeatherBug.com. 2016. Bauchi-Nigeria: Weather Conditions and Forcast [Online]. Available at: http://weather.weatherbug.com/Nigeria/Bauchi-weather.html [Accessed: 14 October 2016].

[12] Climate-data.org. 2016. Climate data for Bauchi [Online]. Avalable at: http://en.climate-data.org/location/46662/Bauchi [Accessed: 13 October 2016].

[13] 2010. NPC, Federal Republic of Nigeria, 2006 Population and Housing Census. Abuja, Nigeria: National Population Commission of Nigeria.

[14] J. R. Jensen and D. C. Cowen. 2011. Remote Sensing of Urban/Suburban Infrastructure and Socio-Economic Attributes. The Map Reader: Theories of Mapping Practice and Cartographic Representation. pp. 153-163.

[15] F. Kruse, K. Kierein-Young, and J. Boardman. 1990. Mineral mapping at Cuprite, Nevada with a 63-channel imaging spectrometer. Photogrammetric Engineering and Remote Sensing. 56: 83-92.

[16] D. A. Roberts, Y. Yamaguchi and R. J. P. Lyon. 1985. Calibration of Airborne Imaging Spectrometer Data to Percent of Reflectance using Field Measurements. in 19th International Symposium on Remote Sensing of Environment, Ann Arbor, Michigan, USA.

[17] J. E. Conel, R. O. Green, G. Vane, C. J. Bruegge, R. E. Alley and B. J. Curtiss. 1987. Airborne Imaging Spectrometer-2: Radiometric spectral characteristics and comparison of ways to compensate for the atmosphere. in 31st Annual Technical Symposium, San Diego, CA, United States.

[18] T. Nguyen. 2015. Optimal Ground Control Points for Geometric Correction Using Genetic Algorithm with Global Accuracy. European Journal of Remote Sensing. 48: 101-120.

[19] J. A. Richards and X. Jia. 1999. Remote sensing digital image analysis, 3rd ed. Berlin: Springer.

[20] J. R. Otukei and T. Blaschke. 2010. Land cover change assessment using decision trees, support vector machines and maximum likelihood classification algorithms. International Journal of Applied Earth Observation and Geoinformation. 12: S27-S31.

[21] R. G. Congalton, R. G. Oderwald and R. A. Mead. 1983. Assessing Landsat classification accuracy using discrete multivariate analysis statistical techniques. Photogrammetric Engineering and Remote Sensing. 49: 1671-1678.